BORNEO JOURNAL OF SCIENCES AND TECHNOLOGY (BJoST)
VOL. : 8, ISSUE: 1, 122-144
DOI: http://doi.org/10.35370/bjost.2026.8.1-11
e-ISSN: 2672-7439, UTS Publisher.

University of Technology Sarawak

ORIGINAL ARTICLE

Hydrogeochemical profiling and suitability evaluation of groundwater for industrial and municipal applications in the Southern Anambra Basin, Nigeria

[1]Kenneth Obinna Iheme, [2,6*]Obinna Chigoziem Akakuru, [3]Hussain Olanrewaju Abubakar, [4]Ayatu Ojonugwa Usman, [1]Mercy Titilayo Alebiosu, [5]Ruben Ibuku Obaro, [1]Michael Chukwudi Olelewe, [1]Omolayo Ajoke Omorinoye

[1]Department of Geology, University of Ilorin, Ilorin, Nigeria.
[2]Department of Chemical and Environmental Engineering, University of Cincinnati, Ohio, USA.
[3]Department of Applied Geophysics, University of Ilorin, Ilorin Kwara State Nigeria.
[4]Department of Physics, Geology and Geophysics, Alex Ekwueme Federal University, Ndufu-Alike, Ikwo, Ebonyi State, Nigeria
[5]Department of Minerals and petroleum Resources Engineering Technology, Kwara state Polytechnic, Kwara State Nigeria.
[6]Department of Geology, Federal University of Technology, Owerri, Imo State, Nigeria.

ABSTRACT - Groundwater's hydrogeochemical properties play a crucial role in determining its suitability for industrial and municipal applications. This study assessed groundwater in the Southern Anambra Basin, Nigeria, by analyzing its physicochemical characteristics and applying hydrogeochemical and industrial water quality indices. A total of fifty-five (55) groundwater samples were systematically collected from boreholes across the study area. Samples were analyzed for key physicochemical parameters, including pH, EC, TDS, major cations (Ca^{2+}, Mg^{2+}, Na^{+}, K^{+}) and anions (HCO_3^{-}, Cl^{-}, SO_4^{2-}, NO_3^{-}). Data were interpreted using Piper, Gibbs, and Gaillardet diagrams, along with saturation indices and chloro-alkaline indices, to identify hydrogeochemical facies and dominant processes. Industrial suitability was evaluated using the Langelier Saturation Index (LSI), Aggressive Index (AI), and Puckorius Index (PI). The study aimed to (1) characterize the hydrogeochemical facies of groundwater in the Southern Anambra Basin; (2) determine the dominant geochemical processes influencing groundwater chemistry; and (3) assess the suitability of groundwater for industrial and municipal systems based on its scaling and corrosive tendencies. The results reveal that groundwater is mainly of the Ca^{2+}+Mg^{2+}–HCO_3^{-} and Ca^{2+}+Mg^{2+}–SO_4^{2-}–Cl^{-} facies, dominated by rock–water interactions. Saturation index values for minerals such as calcite, dolomite, and gypsum were <0, indicating undersaturation and a tendency toward dissolution. LSI, AI, and PI values ranged from −3.22 to −0.03, 8.61 to 11.89, and 3.84 to 8.31, respectively implying a high corrosivity and low scaling potential of groundwater within the study area. These findings suggest that the water poses a corrosion risk to metallic industrial and municipal infrastructure. Mitigation measures such as corrosion-resistant materials and pH adjustment are recommended to preserve system integrity.

ARTICLE HISTORY
Received: 19 Mar 2025
Revised: 24 June 2025
Accepted: 16 Oct 2025

KEYWORDS
Hydrogeochemistry, Water quality assessment, groundwater, Saturation Indices, Langelier Saturation Index.

INTRODUCTION

Water is used in industries for processing, fabricating, washing, cooling, diluting, or transporting a product [1]. Hence, the industrial and economic growth of a region is influenced by the quality of available water in that area [2; 3]. However, the development of large urban areas may result in over-

*Corresponding Author: Author Name. Federal University of Technology (FUTO),
email: Obinna Akakuru; Obinna.akakuru@futo.edu.ng

exploitation/abstraction, as well as a decline in groundwater quality due to the release of polluting substances into them, which alter their chemistry [4 - 6].

Groundwater's hydrogeochemical properties heavily influence its suitability for industrial purposes [7; 8]. Hydrogeochemical approaches are used to identify groundwater facies/type and hence how it has been interacting with the surrounding aquifer materials. Several hydrogeochemical processes account for groundwater chemistry such as rock-water interaction, recharge by precipitation or seawater intrusion, isolated aquifer storage, and mineral species dissolution, oxidation reduction, and biological processes [9]. Hydrogeochemistry also identifies nature and type of ion exchanges, and examines if a mineral species will precipitate or dissolve in a groundwater body, and can also infer the age of groundwater, and if a groundwater is recharges by a stream or a stream is recharged by groundwater [9 - 12].

Several studies have been carried out to investigate the hydrogeochemistry of different parts of the world. [2] carried out a hydrogeochemical characterization of groundwater at Sohag City (Egypt), [13] studied the hydrogeochemical characteristics and evolution mechanism of groundwater in southwestern Ordos Basin, China. [14] investigated the hydrogeochemistry of Lagos State (Nigeria) to determine the water's ionic composition. [15] identify the source of groundwater salinity and the hydrogeochemical process involved in groundwater salinization in the Amol-Babol Plain, Iran. [16] used hydrogeochemistry to identify the hydrogeochemical facies in Eastern Niger Delta. [17] studied the hydrogeochemistry of Uromi and environs, South - South Nigeria. [18] used hydrogeochemistry to find natural processes that influence the chemical composition of groundwater as well as anthropogenic factors that currently affect them in the Dumne Area of Northeast Nigeria. [19] described the hydrogeochemistry of parts of Port Harcourt City (Nigeria) using Piper Trillinear and Gibbs Diagrams and factors governing the chemistry of the area.

Similarly, recent studies across the Niger Delta and adjoining basins have applied integrated geochemical and statistical approaches to decipher groundwater evolution and quality trends. For example, [20] demonstrated the value of machine-learning-driven hydrogeochemical modeling for predicting irrigation suitability in southeastern Nigeria, while [21] employed multivariate statistics and pollution indices to identify anthropogenic contamination near coal-ash dumps. Similarly, [22] examined saline intrusion and hydrogeological dynamics in coastal aquifers of the Niger Delta, emphasizing the link between hydrochemistry and environmental risk. These emerging datasets highlight the increasing relevance of advanced modeling, spatial analytics, and machine learning for improving the interpretation of hydrochemical processes in complex aquifer systems.

On the other hand, corrosion and scaling are the two main properties used to evaluate the industrial usefulness and feasibility of groundwater or surface water for transport in municipal systems within a region. Corrosive water, often referred to as "aggressive water," is water that dissolves materials with which it comes into contact. Corrosion is the physical-chemical interaction between a metal and its surroundings that is usually electrochemical in nature and can cause the metal to change [23]. Furthermore, in Industries and municipal water systems, corrosive water can cause holes in metal plumbing systems, coil pipeline, and metallic parts of machinery [24; 25]. Corrosion causes metal particles to be released from pipes into the fluids. [26]. Corrosion, especially in plumbing systems for urban water supply has the potential to endanger human health due to the possibility of heavy metals such as copper, lead, cadmium, and chromium being released [27]. Similarly, other adverse effects of corrosion include reduced efficiency of hot-water heaters, and cause leaky valves [28].

Water scaling occurs when water contains elevated concentrations of dissolved minerals particularly calcium (Ca^{2+}) and magnesium (Mg^{2+}) ions. As the mineral content increases, the tendency for scale formation also rises. Over time, these mineral deposits accumulate as hard layers along the inner surfaces of pipes, gradually reducing the effective pipe diameter and subsequently decreasing flow rates [26]. Prolonged consumption of water with high scaling potential may pose health risks, including gastrointestinal tract (GIT) disturbances [26]. The predominant component of most scales is calcite ($CaCO_3$), which forms a dense, resistant buildup capable of causing pipe leaks, clogging, and increased maintenance costs [29]. In addition to scaling, corrosion-related effects such as bitter taste, discoloration of laundry, and staining of plumbing fixtures which further deteriorate water quality and household plumbing systems [28].

Water's corrosiveness and scaling tendencies are dependent on several physicochemical parameters. pH, Ca2+ , water temperature, hardness, oxygen, dissolved solid content (TDS), and total alkalinity of water are examples of these [24; 25].Ryznar index (RI), Langelier saturation index (LSI), Puckorius Index (PI) and Aggressive Index (AI) are the standard indices used to evaluate the scaling and corroding tendencies in groundwater, and has been used by several authors [25; 26; 30 - 37] to evaluate the industrial usefulness of groundwater. These indices are simple and to compute and interpret; there are no statistical and mathematical complexities involved [25]. However, in order to avoid unnecessary expenses and working hours, it is critical to have a proper assessment of water quality for industrial purposes [35; 38; 39].

Existing research has extensively explored the hydrogeochemical characteristics of groundwater in various global and regional contexts, often linking groundwater quality to its general suitability for consumption and industrial use. However, studies addressing groundwater suitability for specific industrial and municipal transport systems in the Southern Anambra Basin of Southeastern Nigeria are limited. Given the region's increasing industrial and urban development, a thorough understanding of the groundwater's corrosive and scaling potential is essential to prevent infrastructural damage in industrial and municipal pipelines. The absence of comprehensive analyses specifically targeting these aspects within the Southern Anambra Basin presents a critical research gap, as previous studies primarily focus on drinking water quality or general hydrogeochemical profiles without detailed consideration of the impact on local industrial and municipal water infrastructure.

The primary objectives of this study are to (1) characterize the hydrogeochemical signature of groundwater within the Southern Anambra Basin, Southeastern Nigeria, (2) assess the suitability of the groundwater for industrial and municipal transport systems based on its scaling and corrosive potential, and (3) apply indices such as the Langelier Saturation Index (LSI), Aggressive Index (AI), and Puckorius Index (PI) to evaluate groundwater quality for corrosion and scaling tendencies. Additionally, the study will aim to identify the dominant hydrogeochemical processes, such as rock-water interactions and mineral dissolution patterns, that influence groundwater composition and assess the implications of these processes on groundwater quality for industrial applications.

The novelty of this study lies in its focused approach to evaluating groundwater for industrial and municipal applications within the Southern Anambra Basin, using a robust suite of hydrogeochemical indices tailored to assess corrosion and scaling potential. Unlike previous studies that have generalized groundwater quality for consumption, this research provides critical insights into the implications of water chemistry on infrastructure longevity in an industrial setting. By addressing this gap, the study offers practical recommendations for water management strategies that can mitigate corrosion-related damage, optimizing water quality and infrastructure reliability for industrial stakeholders in Southeastern Nigeria.

MATERIALS AND METHODOLOGY

Location and Geology

The study area is located in Imo State, Southeast Nigeria, between latitudes 5°38'0" to 5°46'0" N and longitudes 6°56'0" to 7°8'0" E, covering approximately 244 km² (Figure 1). It is centered in Isu and includes the Local Government Areas of Orlu, Njaba, Oru East, Oru West, Mbaitoli, Ikeduru, Isiala Mbano, Nwangele, and Nkwerre. The area is accessible via several major roads, including the Owerri-Orlu Road, Nkwerre Road, and the Onitsha-Owerri Expressway. The main rivers that drain the region are the Njaba and Okitankwo Rivers. Geologically, the study area is situated within the southern part of the Anambra Basin. The predominant rock types are sandstones with thin interbedded clay and shale units, belonging to the Benin Formation, Ogwashi-Asaba Formation, and Ameki Formation (Figure. 2).

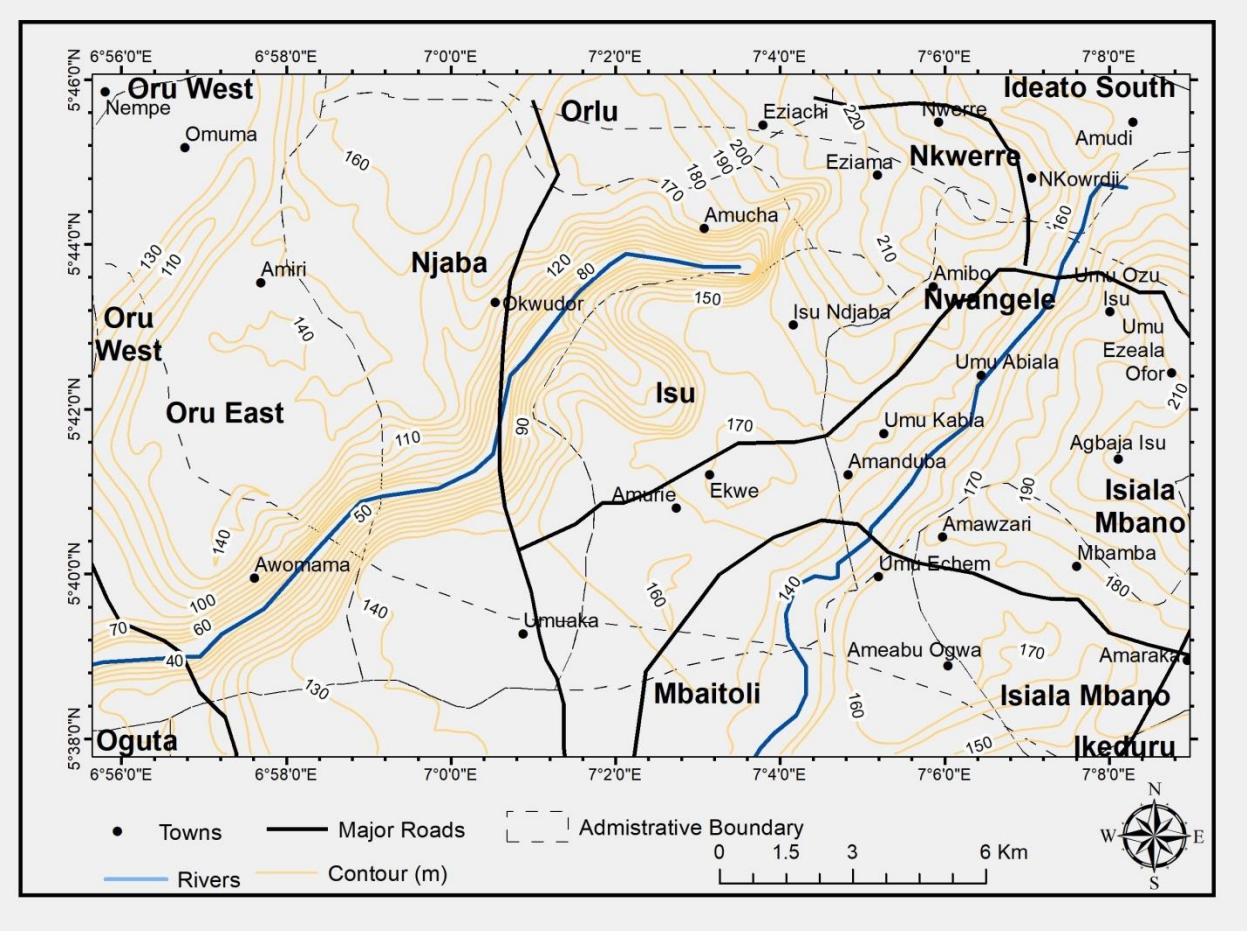

Figure 1. Location of the study area

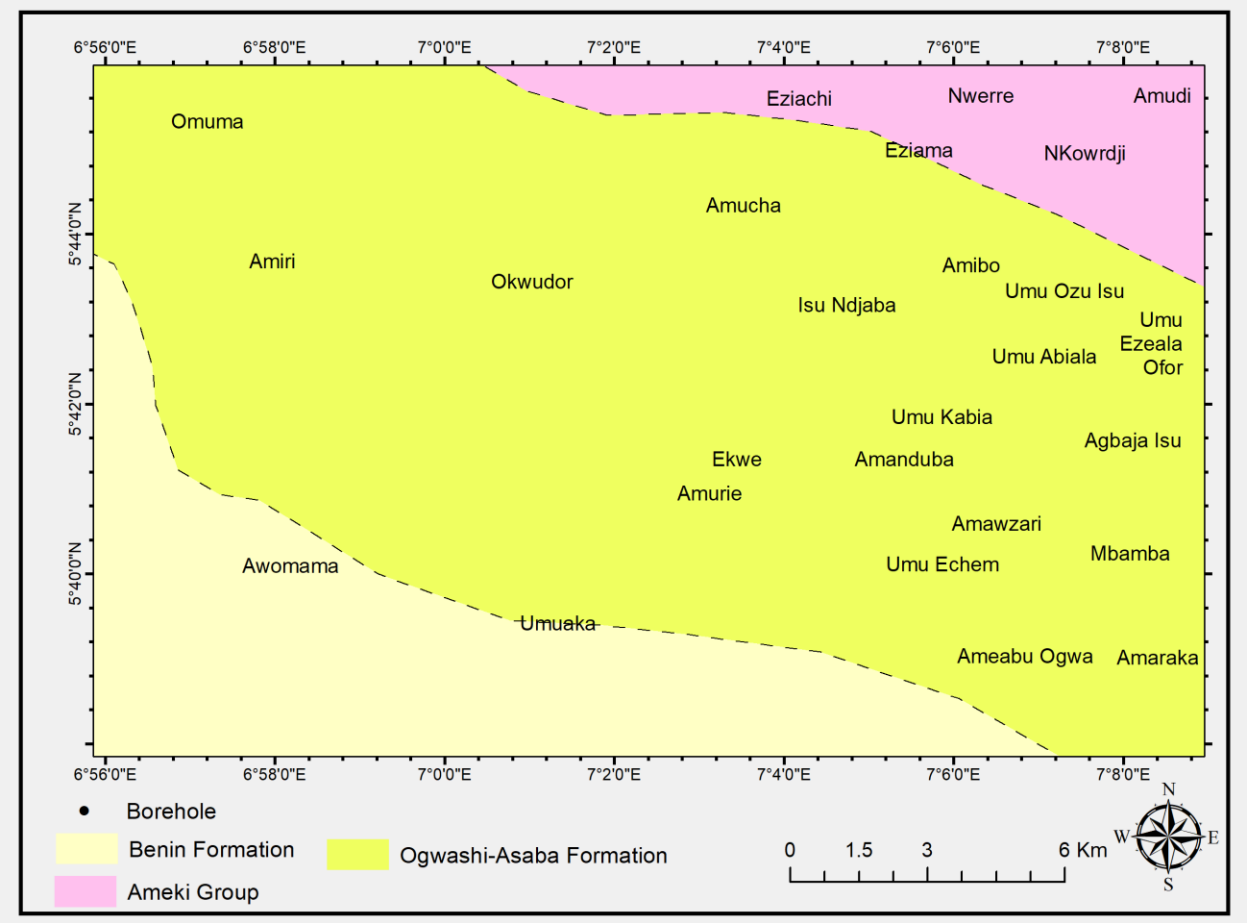

Figure 2. Geology of the study area

Sampling and Laboratory Procedures

Fifty-five (55) water samples were taken from boreholes located throughout the study area. All containers used for sampling were cleaned with deionized water both before and after use to prevent sample contamination. Handheld instruments used for in-situ physical property measurements were also cleaned and calibrated. Boreholes were flushed beforehand to eliminate stagnant water, ensuring that water extracted came directly from the aquifer. The sampling containers were rinsed with water from the borehole before being filled. Samples for cation determination were acidified with HNO_2 to a pH of 2 to maintain cation stability and prevent adherence to the container surfaces. The samples were then kept on ice and stored at 4°C in a refrigerator until analysis. Laboratory analysis of the groundwater samples was conducted with the assistance of a chemist. Physical parameter measurement for pH, total dissolved solids (TDS), electric conductivity (EC), Turbidity (Turb) and Temperature were done in situ during the sampling program using various handheld meters. In the laboratory, the samples were chemically examined for dissolved oxygen (DO), chloride (Cl^-), total alkalinity (Alk), nitrate (NO_3^-), sulphate (SO_4^{2-}), calcium (Ca^{2+}), bicarbonate (HCO_3^-), sodium (Na^+), Magnesium (Mg^{2+}), potassium (K^+) and carbonates (CO_3^{2-}).

Interpretation of Result

Summary/descriptive statistics, and comparison with recommended standards limits for drinking water etc. were applied on the hydrogeochemical datasets. Piper diagram and Durov diagram were used to identify the hydrogeochemical facies or the dominant ions that control the groundwater chemistry of the area. Gibbs diagram, Gaillardet End Member diagram, chloro-alkaline indices, and saturation index were used to define the hydro-geochemical processes and the character of ionic exchange in the study area's groundwater.

The spatial variation of major ion chemistry in the study area was depicted using inverse distance weighted interpolation**.** Inverse Distance Weighting (IDW) interpolation is a mathematical (deterministic) spatial interpolation technique that assumes closer points/locations are more related than further points within its function. Spatial interpolation creates surfaces by estimating unknown points from known points data. The spatial autocorrelation that underlies IDW is the assumption that near points are more alike than points which a further away (Tobler's First Law of Geography). IDW is very flexible in the sense it can use fixed number of values or variable points within a search ellipse. Another reason IDW interpolation is so versatile is that it can capture linear geologic/geographic features such as fault lines [40]. IDW is more effective when estimation is done within a convex hull. Surfer 18 software was used to produce the IDW map of the computed industrial water quality indices in this study.

The Piper diagram [41] is used to visualize the relative abundance of common ions in water samples, allowing water samples to be grouped based on groundwater facies and other criteria. A piper plot is comprised of three components: a ternary diagram in the lower right representing anions (sulfate, chloride, and carbonate plus bicarbonate), a ternary diagram in the lower left representing cations (calcium, magnesium, and sodium plus potassium), and a diamond plot in the middle which is a matrix transformation of the two ternary diagrams. The top quadrant of the piper diagram's diamond plot contains calcium-magnesium-sulfate-sulfate waters (permanent hardness), the left quadrant contains calcium bicarbonate waters (shallow-fresh groundwaters), the right quadrant contains sodium chloride waters (marine and deep ancient ground waters), and the bottom quadrant contains sodium-bicarbonate waters (deep ground water influenced by ion exchange.)

Durov diagram [42] is a data visualization technique in hydrogeology which displays the major ions as percentages in milli-equivalents in two trilinear graphs that form additional two-dimensional projections (The Durov projection). Since the percentages of the anion and cation groups are forced to 100%, when interpreting one need to look at the dominant cation and anion species. Samples that form clusters on the Durov projection are assumed to be of similar chemical composition of major anion and cation [43]. In the central rectangle, [44] classified nine fields. According to[45], the importance of each field is as follows: field 1 (HCO_3^- and Ca^{2+}-dominated) frequently implies recharging waters in sandstones, limestones, and many other aquifers; field 2 (HCO_3^- and Mg^{2+} or Ca^{2+}/Na^+ indiscriminate) and field 3 (HCO_3^- and Na^+ dominant) indicate ion-exchange waters; fields 4 and 5 shows waters exhibiting simple dissolution or mixing; field 6 indicates probable mixing influence; fields 7 and 8 indicate reverse ion-exchange reactions; and field 9 represents end point waters. Bivariate plots were used to identify patterns in the ratios of specific anions and cations, helping to determine whether the water from different wells originates from a common or distinct source [46].

Although the Gibbs Diagram [47] was designed to identify processes controlling surface water chemistry, several authors have used it to study processes controlling groundwater chemistry [48; 49; 50; 51]. Groundwater and surface water systems are constantly interacting when water enters an aquifer from a flowing stream and vice versa. The strong ground-to-surface interaction highlights the fact that even surface waters are partially 'groundwaters' [52]. Gibbs diagram consist of total dissolved solids (salinity) on the y-axis plotted against $Na^+/(Ca^{2+}+Na^+)$ ratios or $Cl^-/(Cl^- + HCO_3^-)$ ratios (x-axis). Gibbs diagram identifies the governing processes (evaporation, precipitation, and water-rock interaction) which control groundwater chemistry [53].

Gaillardet end-member diagram [54] is used to characterize the nature of rock-water interaction/chemical weathering of various lithological facies (silicate rocks, carbonate rocks and evaporitic rocks).Gaillardet end-member diagram based on molar ratio relationships (Mg^{2+}/Na^{+}, Ca^{2+}/Na^{+}, HCO_3^{-}/Na^{+}). This method is based on the idea that the chemical composition of water carries a unique signature associated with each altering rock, as defined by ionic ratios that are conservative during evaporation and dilution processes. Depending on the lithological facies within a basin, the river water composition results from the simple combination of these weathering signatures [55 - 57].

The chloro-alkaline indices (CAI-1 and CAI-2) are widely used to evaluate the nature of ion exchange responses between groundwater and surrounding aquifer materials during residence or travel, and are calculated using [58]'s Equations 1 and 2. Positive Chloro-Alkaline Indices indicate that Na^{+} and K^{+} from the water are exchanged with Mg^{2+} and Ca^{2+} from the rocks, whereas negative indices indicate that Mg^{2+} and Ca^{2+} from the water are exchanged with Na^{+} and K^{+} from the rocks [59].

Mineral reactivity in an aquifer is measured using saturation indices (Equation 3). The saturation index (SI) for a specific mineral indicates whether groundwater is undersaturated (SI < 0), at equilibrium (SI = 0), or supersaturated (SI > 0) with respect to that mineral. If groundwater is undersaturated with respect to a mineral, as indicated by a negative SI, the mineral should theoretically dissolve. In contrast, if groundwater is supersaturated with a mineral, the mineral will theoretically precipitate from the groundwater [60]. SI was calculated using the geochemical program PHREEQC [61].

All the geochemical diagrams were produced using R Version 3.5 with extension packages GQAnalyzer and jentjr/gwstats. GQAnalyzer was used to produce Piper and Durov diagrams. Gibbs, End-member, and bivariate and other bivariate plots were produce using base R. The bivariate diagrams were color coded based on the classes identified on the Piper diagram. The maps showing the spatial distribution of some of the parameters was done in Surfer 18.

$$CAI\text{-}1 = Cl^{-} - (Na^{+} + K^{+})/Cl^{-} \quad (1)$$

$$CAI\text{-}2 = Cl^{-} - (Na^{+} + K^{+})/(SO_4^{2-} + HCO_3^{-} + CO_3^{2-} + NO_3^{-}) \quad (2)$$

$$SI = \log(IAP/Ksp) \ . \quad (3)$$

Table 1. Industrial water quality indices and classification ranges

Index	Equation	Classification and interpretation
Langelier Saturation index (LSI)	LSI = pH – pHs	-3.0> LSI > -5.0 Very Severe Corrosion -1.0> LSI >-3.0Moderate Corrosion -1.0 >LS1 >1.0Balance 1.0 < LSI < 3.0Moderate Scale 3.0 < LSI < 5.0Very Severe Scale
Aggressive index (AI)	$AI = pH + Log_{10}(Alk * Ca^{2+})$	AI > 12 Water has scaling property 10 < AI < 12 water is approximately corrosive AI<10 water is very aggressive
Puckorius index (PI)	PI = 2pHs – pHeq	PI < 6: Water with a scaling tendency 6 ≤ PI ≤ 7: Water with little scaling and corrosive tendencies PI > 7: Water with a significant corrosive tendency

$$pHs = (9.3+A+B) - (C+D) \quad (4)$$

$$pHeq = 1.465 \times Log_{10}(Alk) + 4.54 \quad (5)$$

$$A = (Log_{10}(TDS)-1)/10 \quad (6)$$

$$B = -13.12 \times Log_{10}(T + 273) + 34.55 \quad (7)$$

$$C = Log_{10}(Ca^{2+})-0.4 \quad (8)$$

$$D = Log_{10}(Alkalinity\ as\ CaCO3) \quad (9)$$

To assess the corrosion and scaling potential of groundwater systems in the study area, the Langelier saturation index (LSI), Aggressive Index (AI) and Puckorius index (PI) were used. Table 1 shows the equations used to calculate these indices, where pHs is the pH of water in the saturated state of calcium carbonate and pHeq is the pH at equilibrium. Equations 4-9 show how pHs and pHeq are computed from basic groundwater parameters which includes alkalinity (Alk), total dissolved solids (TDS), temperature (T), Calcium concentration (Ca^{2+}). The unit of measurement for Alk, TDS, Ca^{2+} are in mg/L is, and temperature is measured in degree Celsius.

RESULTS AND DISCUSSION

Concentrations of Chemical Constituents of Groundwater

Groundwater parameter summary statistics and comparison with World Health Organization standards [62] are presented in Tables 2. Temperature, EC, Turbidity, DO, Alkalinity, Ca^{2+}, Mg^{2+}, Na^{+}, HCO_3^{-}, and SO_4^{2-} are below the guidelines set by WHO for potable water in all the samples. pH (44), TDS (2), K^{+} (3), CO_3^{-} (3), Cl^{-} (1), and NO_3^{-} (1) are more than WHO stated values for drinking water in some of the samples.

The pH level in groundwater samples ranges from 3.6 to 8.4, with 44 (80%) falling below the WHO recommended range of 6.5-8.5 for potable water and indicates largely acidic groundwater. Previous studies of groundwater from Nnewi, Awka, and Umunya within the Anambra Basin, also revealed that a significant proportion of the samples were acidic [63; 64]. The acidic nature may be attributed to infiltration on the acid rain into the groundwater system, and percolating surface water encountering decaying organic matter before joining the underlying aquifer in the area. The aquifer materials are silicates sandstone layers of Benin, Ogwash-Asaba and Ameki Formatios and are devoid of limestones which could raise the pH level. However, the acidic nature of groundwater does not have negative health implications for humans but may however alter the taste of the groundwater if in excess [65; 66; 64]. The groundwater samples have Temperature, EC, TDS Turbidity, DO, Alkalinity values that range from 23.5 to 31.6^{o}C, 13 to 889µS/cm, 8.45 to 557.9mg/L, 0.05 to 4.1NTU, 3.1 to 7.7mg/L, and 34 to 590mg/L respectively. TDS are high in 2 (two) samples which can be attributed to localized high dissolution/leaching of ions.

The HCO_3^{-} concentrations in the groundwater samples ranged from 24 to 580 mg/L, with a mean concentration of 145.13 mg/L. Weathering of carbonate and alumino-silicate rocks is a common source of HCO_3^{-} [67]. Figure 3d depicts the regional distribution of HCO_3^{-} as higher values interrupting a pattern of low values. The concentration of SO_4^{2-} ranges from 1 to 40 mg/L, with an average of 9.56 mg/L. All of the SO_4^{2-} concentrations are below the WHO desirable drinking limit. Figure 3f shows that the western half of the area has higher SO_4^{2-} values than the eastern half. The concentration of Cl^{-} varies between ND and 285 mg/L (average: 40.86 mg/L). The spatial distribution of Cl^{-} is depicted in Figure 3e. The concentrations of NO_3^{-} range from 0.4 to 44 mg/L, with an average of 2.71 mg/L. One (1) sample contained more NO_3- than the WHO permissible limit of 10 mg/L. Higher NO_3^{-} levels in groundwater may be caused by agricultural or other anthropogenic activities in the vadose zone [68]. The average anion inequality of groundwater samples is HCO_3^{-}>Cl^{-}> SO_4^{2-}>NO_3^{-}.

Ca^{2+} levels range from 0.22 to 65mg/L, with an average of 29.13 mg/L. The regional distribution map of Ca^{2+} (Figure 3a) shows that higher Ca^{2+} values formed a boomerang belt originating in the west and moving east. The concentrations of Mg^{2+} range from 0.09 to 49.50 mg/L, with an average of 13.59 mg/L. Figure 3c depicts the distribution of Mg^{2+} in the study area. The concentrations of Na^{+} range from 2.26 to 30 mg/L, with an average of 13.95 mg/L. Figure 3b shows that the highest concentrations of Na^{+} are found on the study area's south-eastern flank. K^{+} concentrations range from 0.01 mg/l to 100 mg/l, with a mean of 7.85 mg/l.

The combination of low scaling potential and high corrosivity presents a unique and critical risk to groundwater-dependent industrial and municipal systems. While low scaling typically reduces mineral deposition within pipelines, high corrosivity indicates a strong tendency for metal dissolution and infrastructure degradation. In such environments, the absence of protective scale films commonly composed of calcium carbonate—allows direct and accelerated corrosion of metallic components. This condition leads to pitting, leakage, and structural weakening of pipes, storage tanks, and distribution systems. Unlike scaling-dominant systems, where mineral crusts can act as partial barriers to corrosion, the chemically aggressive groundwater in the Southern Anambra Basin lacks such self-protective characteristics. Consequently, prolonged exposure can result in frequent maintenance cycles, increased operational costs, and compromised water quality due to the release of metallic ions. Therefore, the concurrent presence of low scaling and high corrosive potential should be regarded as a high-priority geochemical hazard, necessitating proactive mitigation strategies such as the use of non-metallic or corrosion-resistant materials, pH stabilization, and chemical conditioning to prevent infrastructure deterioration and ensure sustainable groundwater utilization.

Table 2. Summary statistics for chemical constituent concentrations in groundwater from Imo, SE Nigeria.

Parameters (unit)	Total samples	Range	Average	Std.dev	WHO (2013)	Number of samples above WHO [62]
pH	55	3.6 - 8.4	5.94	0.9	6.5 - 8.5	44
Temp (^oC)	55	23.5 - 31.6	27.8	1.7	-	-
EC (µS/cm)	55	13 - 889	122.07	179.13	1400	-
TDS (mg/L)	55	8.45 - 557.9	78.59	113.3	500	2
Turbidity (NTU)	55	0.05 - 4.1	0.9	0.68	5	-
DO (mg/L)	55	3.1 - 7.7	5.9	1.41	-	-
Alk (mg/L)	55	34 - 590	155.13	174.08	-	-
Ca^{2+} (mg/L)	55	0.22 - 65	29.13	22.95	75	-
Mg^{2+}(mg/L)	55	0.09 - 49.5	13.59	14.17	50	-
Na^{+} (mg/L)	55	2.26 - 30	13.95	10.11	200	-
K^{+} (mg/L)	55	0.01 - 100	7.85	22.94	50	3
HCO_3^- (mg/L)	55	24 - 580	145.13	174.08	1000	-
CO_3^{2-} (mg/L)	55	12 - 1320	168.85	202.86	500	3
Cl (mg/L)	55	ND - 285	40.86	48.88	250	1
SO_4^{2-}(mg/L)	55	1 - 40	9.56	8.58	400	-
NO_3^- (mg/L)	55	0.4 - 44	2.71	5.8	10	1

*Note: ND =Not detected

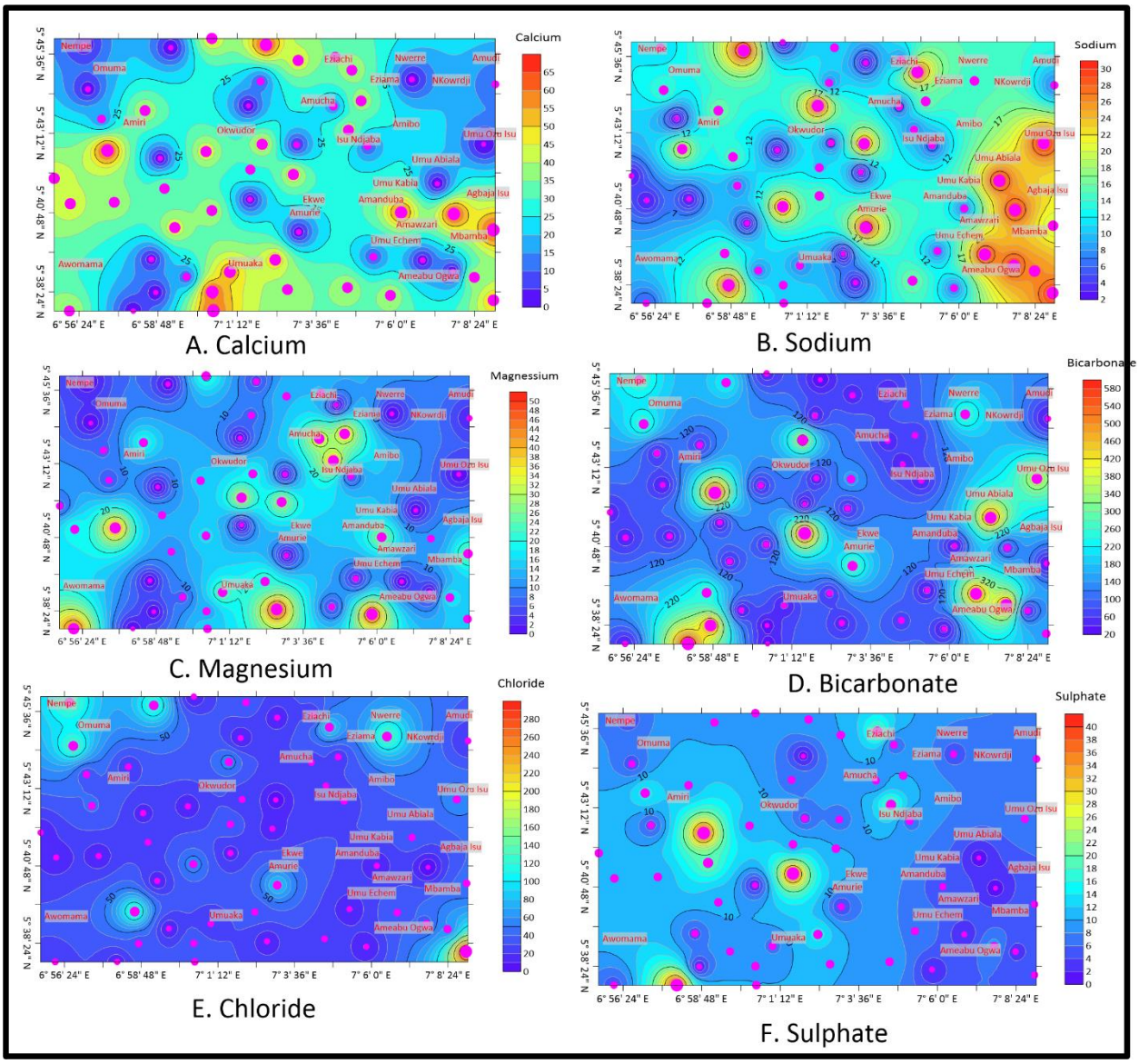

Figure 3. Iso-concentration maps showing regional distribution of Ca^{2+} (a), Na^{+} (b), Mg^{2+} (c), HCO_3^{-} (d), Cl^{-} (e) and SO_4^{2-} (f) in the study area

Hydrogeochemical facies

The Piper diagrams for groundwater samples from different geological formations (Figure 4) reveal that in the Ogwashi-Asaba Formation (Figure 4a), 50% of the samples on the cation ternary are dominated by Ca^{2+}, while 55% are HCO_3^{-}-dominated on the anion ternary. The central diamond shows 90% of samples fall into alkaline earth-dominated fields, with 48.4% in the Ca^{2+}+Mg^{2+}-HCO_3^{-}facies and 41.9% in the Ca^{2+}+Mg^{2+}-SO_4^{2-}-Cl^{-} facies. In the Benin Formation (Figure 4b), 66.67% of groundwater samples are Ca^{2+}-dominated, and 63.64% are HCO_3^{-}-dominated, with all samples falling into the alkaline earth-dominated field; 61.54% are in the Ca^{2+}+Mg^{2+}-HCO_3^{-} facies and 38.46% in the Ca^{2+}+Mg^{2+}-SO_4^{2-}-Cl^{-} facies. The Ameki Formation (Figure 4c) shows Ca^{2+}+Mg^{2+}-SO_4^{2-}-Cl^{-} and Ca^{2+}+Mg^{2+}-HCO_3^{-} as the dominant facies, with most samples falling within alkaline earth and strong acid radical-dominated fields. Overall, groundwater samples across these formations exhibit similar trends, predominantly featuring

Ca^{2+}+Mg^{2+}-HCO_3^- and Ca^{2+}+Mg^{2+}-SO_4^{2-}-Cl^- facies, with regional variations supported by previous studies [69; 70; 71; 72].

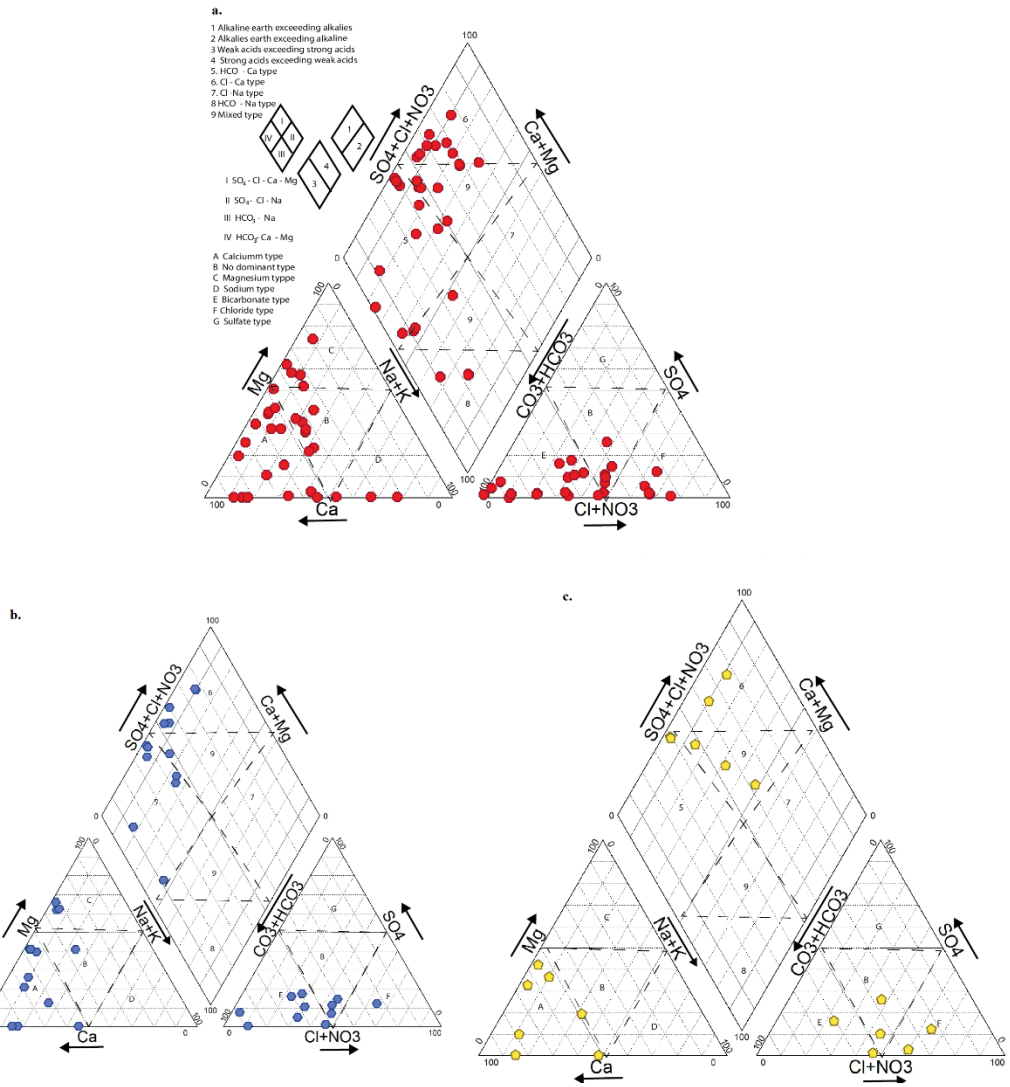

Figure 4. *Piper Diagram depicting hydrogeochemical facies of the groundwater samples based on geological formations (a) Ogwashi-Asaba Formation, (b) Benin Formation, and (c) Ameki Formation*

The Durov diagram for groundwater samples from different geological formations (Figure 5) reveals that most samples plot within the first three fields of [44], with Ca^{2+} as the dominant cation across all formations. On the anion ternary diagram, the Ogwashi–Asaba Formation is dominated by SO_4^{2-}, followed by HCO_3^- (Figure 5a), while the Ameki Formation displays nearly equal influence from SO_4^{2-} and HCO_3^- (Figure 5c). The Benin Formation, on the other hand, is characterized predominantly by HCO_3^- (Figure 5b). On the Durov square, the Ogwashi–Asaba samples suggest a combination of $CaSO_4$ and simple dissolution processes, while the Benin Formation samples are mainly of $Ca(HCO_3)_2$ type, reflecting recent recharge and carbonate mineral dissolution within the aquifer system. However, this hydrochemical signature may also indicate interaction with carbonate-bearing units or limestone lenses, rather than exclusively implying recharge through sandstone aquifers. The Ameki Formation samples exhibit mixed $CaSO_4$–$Ca(HCO_3)_2$ water types, consistent with transitional geochemical evolution. Similar

dilution and mixing trends were reported by [73] and [63] in the Nanka Sands of the Ogwashi–Asaba Formation.

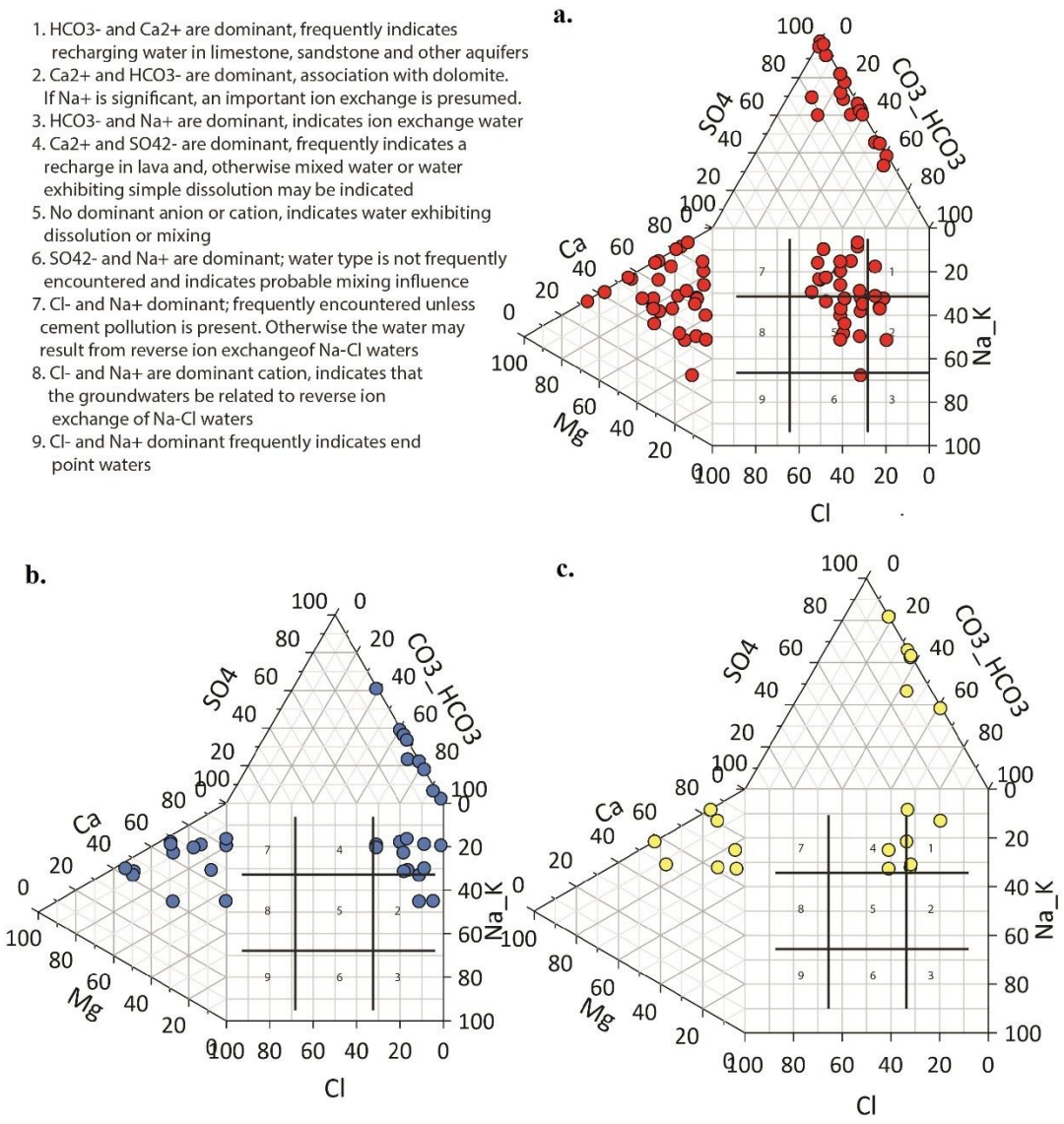

Figure 5. Durov diagram of the groundwater samples based on geological formations (a) Ogwashi-Asaba Formation, (b) Benin Formation, and (c) Ameki Formation

Hydrogeochemical Process

The Gibbs diagram (Figure 6) shows that the majority of the groundwater samples are interacting with rocks and precipitating. This demonstrates how rock-water interaction and precipitation (recharge from rainfall) processes have influenced groundwater evolution in the study area. The ionic ratios on the Gibbs diagram for $Cl^-/(Cl^- + HCO_2^-)$ levels ranged from 0.03 to 0.62, while $Na^+/(Na^+ + Ca^{2+})$ levels ranged from 0.03 to 0.61.

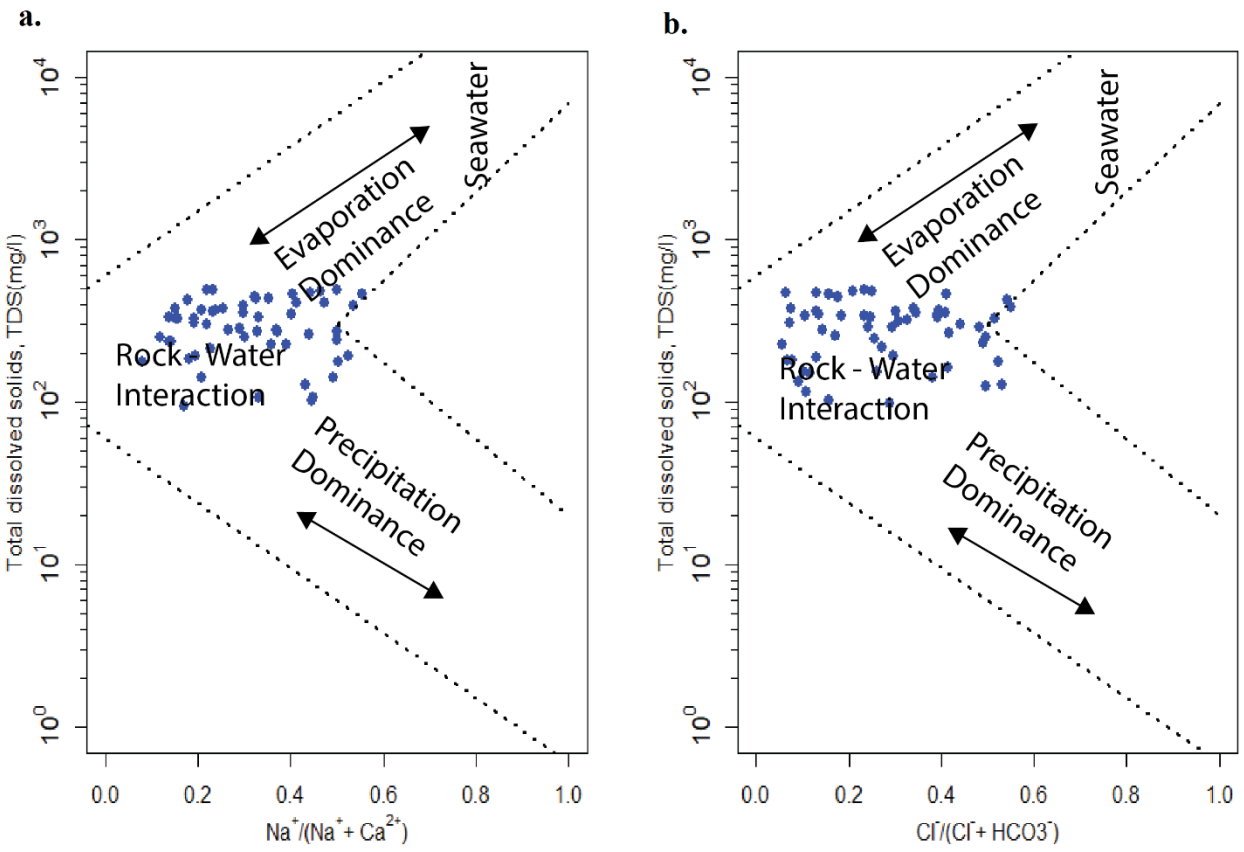

Figure 6. Gibbs diagram of the groundwater sample; (a) cation (b) anion

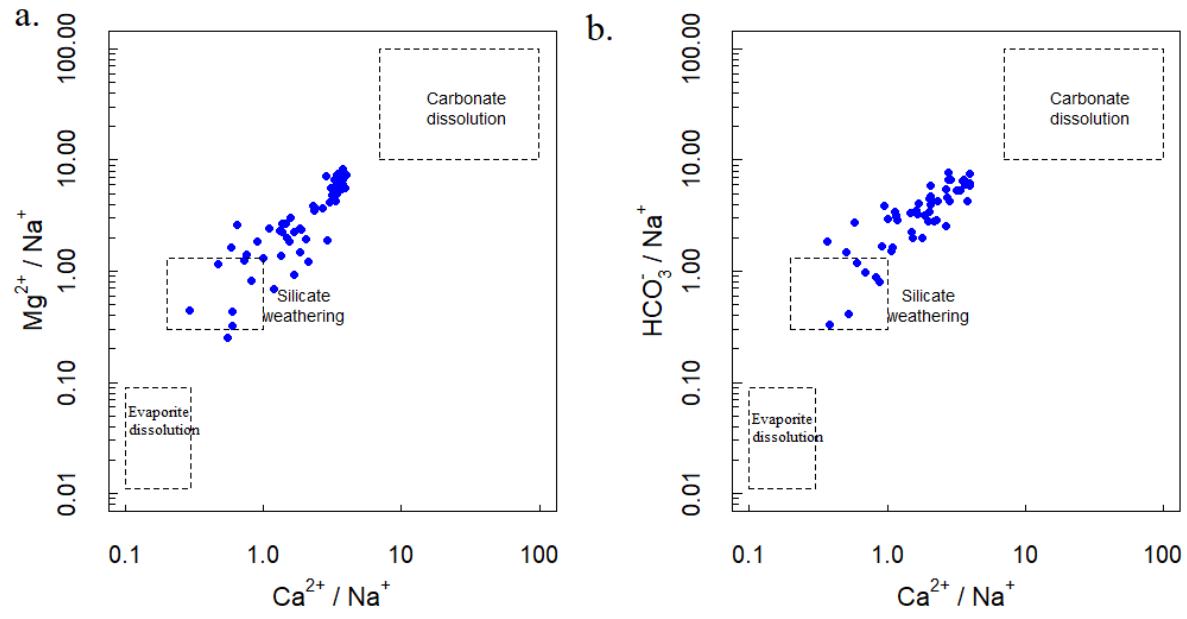

Figure 7. Gaillardet end-member diagram

The Gaillardet end-member diagram of the study area (Figure 7) reveals that most groundwater samples align with the silicate weathering and carbonate dissolution trend. This alignment may be due to variability in the silicate end-member composition and differences in silicate lithological facies, which could extend beyond the typical range of this endmember [57]. The mean molar ratios for HCO_3^-/Na^+, Mg^{2+}/Na^+, and Ca^{2+}/Na^+ on the plot are 4.257, 4.95, and 5.73, respectively. These findings suggest that both silicate weathering and carbonate dissolution play significant roles in the geochemical processes affecting the groundwater in the study area.

The median values of CAI-II and CAI-I are -0.05 and -5.32 respectively. Figure 8 depicts the relationship of CAI-I and CAI-II to distinguish the ion exchange process. It can be observed that 100% of the samples fall on the bottom left of the plot, indicating normal ionic exchange, which results in Na^+ enrichment in groundwater. This finding is consistent with a study of groundwater from the Umunya region in the Anambra Basin, where most samples also exhibited normal ionic exchange, although some showed reverse reactions [63].

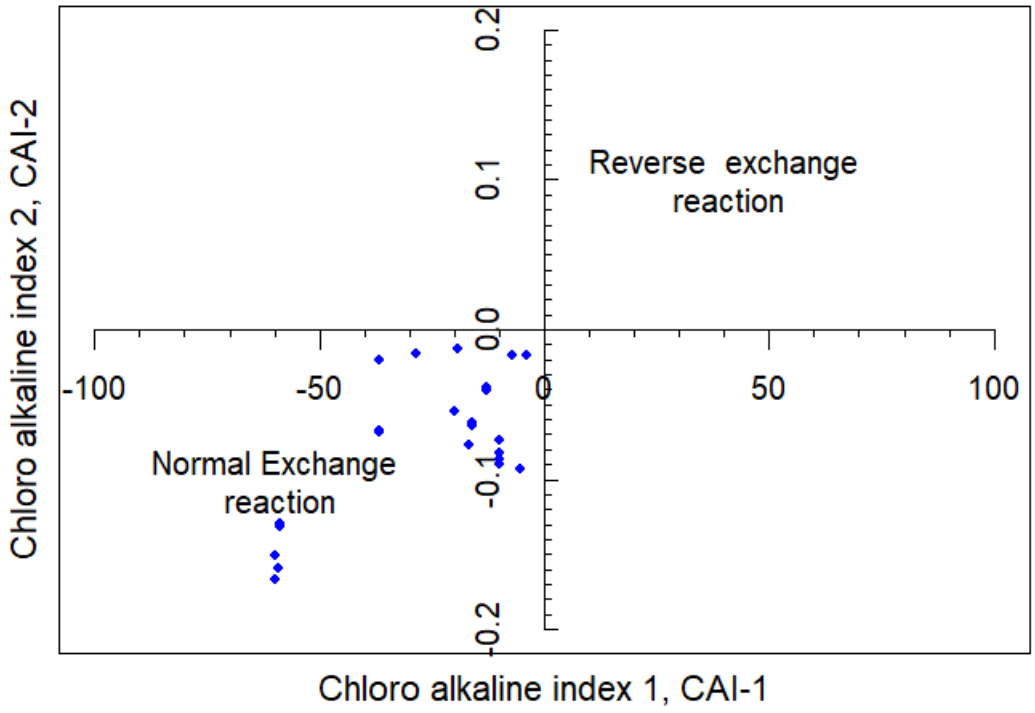

Figure 8. Chloro-alkaline indices (CAI-II versus CAI-I) bivariate of groundwater samples

Figure 9a shows that the SI for Calcite, Dolomite, Aragonite, Anhydrite and Gypsum in all the groundwater samples from the study area are below zero, indicating that groundwater is under-saturated and has a possibility of dissolving. The general trend of SI in the samples is Calcite>Aragonite>Dolomite>Gypsum>Anhydrite which implies that anhydrite is more likely to dissolve than calcite. The saturation index for calcite, aragonite, dolomite, gypsum, and anhydrite varies from -2.4 to -0.54, -2.64 to -0.69, -4.38 to 1.23, -5.67 to-2.35, and -5.89 to -2.57 respectively. Figure 9; bis a boxplot that shows the median values of SI for the considered mineral species follows the order Calcite>Aragonite>Dolomite>Gypsum>Anhydrite.

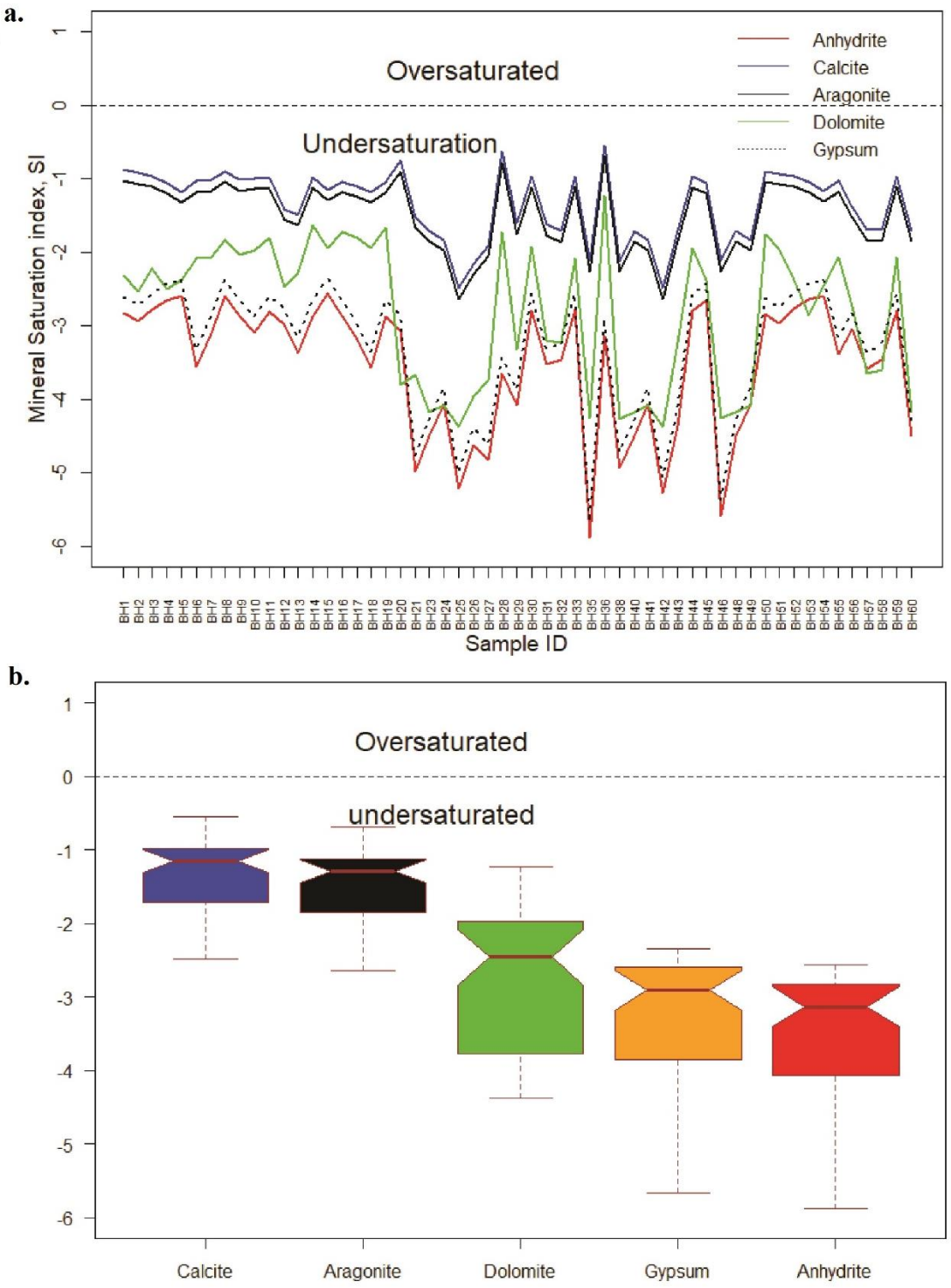

Figure 9. Saturation index distribution (a) for Calcite, Aragonite, Dolomite, Gypsum, and Anhydrite for all groundwater samples in the study area, and boxplot (b) showing the minimum, maximum, median, 1st and 3rd quartile SI in the dataset

Figure 10a presents the ion connection between Cl^- and Na^+ (Na^+/Cl^-). Some of the groundwater samples were located along the 1:1 trend line, and the other samples mostly lay above the 1:1 trend line, implying that halite dissolution, cation exchange and silicate weathering are significant sources of Na^+ [74]. Figure 10b clearly show that most of the groundwater samples lie below the 1:1 trend line of $Ca^{2+}+Mg^{2+}$vs. $HCO_3^-+SO_4^{2-}$ bivariate, implying the effects of the inverse cation exchange process 74]. This chemical process is further outlined in Figure 10c, which shows that most of the samples plotted near or above the 2:1 line of Ca^{2+} + Mg^{2+}vsMg^{2+}. bivariate and could be attributed to dolomite weathering [75]. Figure 10d shows that all the groundwater samples are above the 1:1 line of Ca^{2+}Vs. Ca^{2+} + SO_4^{2-} bivariate, indicating gypsum dissolution [75]. Figure 10e shows that many of the samples are below the total cation Vs Na^+ + K^+bivariate 1:2 line indicating that reverse exchange reactions and silicate weathering are associated in the geochemical process [13]. The ratio of $Cl^-/(HCO_3^- + CO_3^{2-})$, known as the Revelle index (RI), with ion concentrations expressed in meq/L, indicates that salinization affects groundwater when RI values exceed 0.5 [76]. Figure 10f shows that all but one of the groundwater samples plots above the 1:1 line which is suggestive of no salinization.

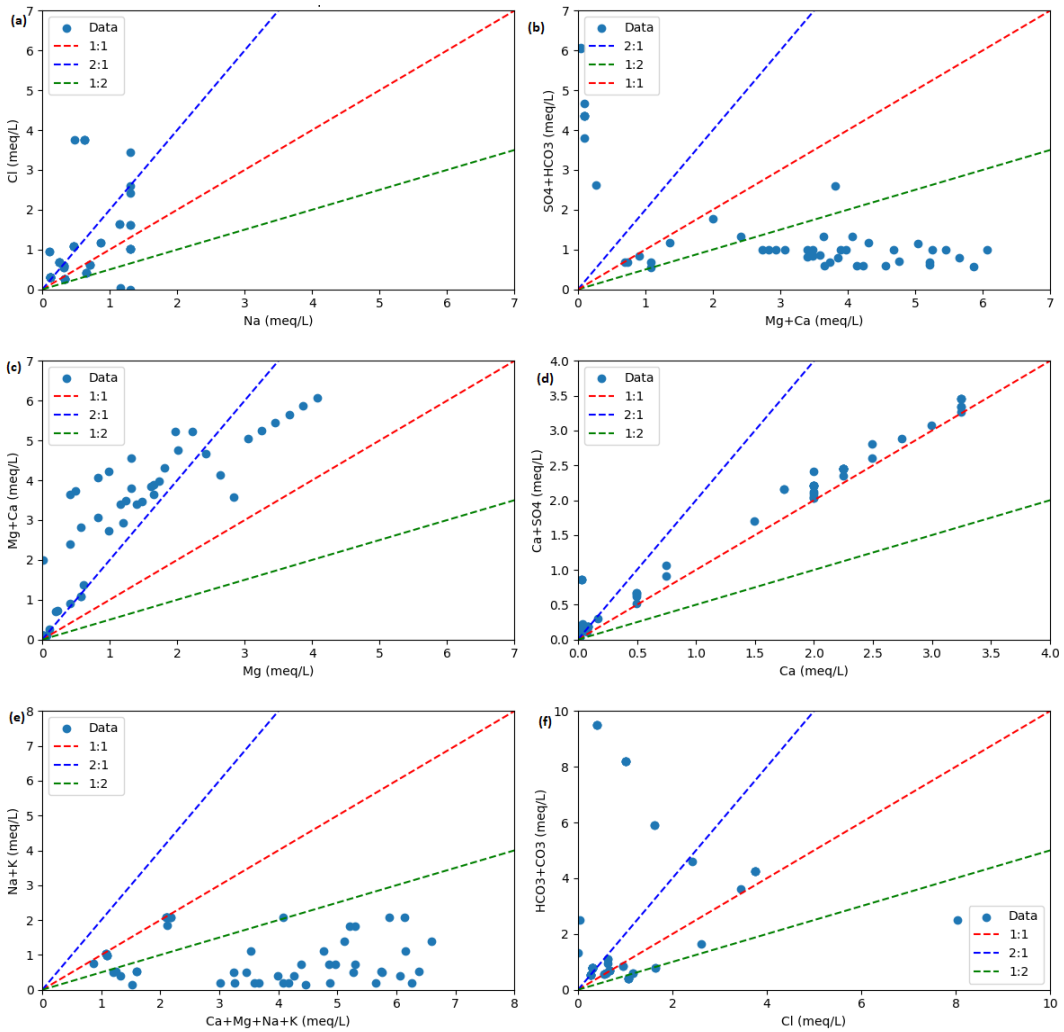

Figure 10. Scatter plots depicting the relationship of major cations/anions to differentiate geochemical processes. (a) Na^+ vs. Cl^-, (b) $Ca^{2+}+Mg^{2+}$vs. $HCO_3^-+SO_4^{2-}$ (c) Mg^{2+}vs. Ca^{2+} + Mg^{2+} (d) Ca^{2+} Vs. Ca^{2+} + SO_4^{2-} (e) Total Cation VS Na^+ + K^+ (f) Cl^- VS $HCO_3^-+CO_3$

Industrial and Municipal Systems Water Quality Assessment

Table 3 displays the descriptive statistics for the various computed industrial water quality indices. Figure 11a shows the distribution of Langelier saturation index (LSI) in groundwater samples from the study area. LSI values typically range between -3 and + 3, with negative values representing under saturated water with a corroding tendency [35]. The maximum and minimum values of LSI were observed at BH8 (-0.03) and BH26 (-3.22) respectively. LSI classifies water into three categories: very severe corrosion (1.82%), moderate corrosion (63.64%), and balance (34.55%). The corrosive tendencies could be explained by the low pH values observed.

The distribution of Aggressive Index (AI) values in water samples reveals minimum and maximum values of 8.61 and 11.89, respectively, with a mean of 10.61 ± 0.74 (Figure 11b). 83.64% of the water samples (46 out of 55) are severely corrosive while 16.36% (9 out of 55) are approximately corrosive. The Puckorius Index (PI) for water scaling tendencies ranges from 3.8 to 8.31, with an average of 6.31 ± 1.04. The classification shows that 32.73% of the water has a scaling tendency, 41.82% exhibits both minor scaling and corrosive tendencies, and 25.45% shows a significant corrosive tendency (Figure 11c). The findings of this study are consistent with a previous study on groundwater in the Anambra Basin, which found it to be severely corrosive and potentially damaging to metallic municipal water distribution systems [77; 10; 11; 12]. However, the AI (Aggressiveness Index) was originally designed for monitoring water in asbestos pipes [78] and may not be a reliable indicator of groundwater corrosivity in relation to metallic water distribution systems.PI considers the maximum amount of calcium carbonate that can precipitate when the water reaches equilibrium [79]. Given the PI values observed in this study, it is evident that the groundwater has a low capacity for forming protective calcium carbonate scales, leaving metallic water distribution systems vulnerable to corrosion and exacerbating the risk of damage to infrastructure.

Mitigating the high corrosive tendency of groundwater in industrial and municipal water systems involves installing corrosion-resistant plumbing components, such as approved plastic PVC pipes. Additionally, treatment units like neutralizing filters or chemical feed systems can be installed at the Point-of-Entry (POE) of water delivery systems to households. These systems work by adding alkaline chemicals to the water, effectively reducing its corrosivity. Acid-neutralizing filters, such as calcium carbonate (limestone) chips, magnesium oxide, marble chips, or other alkaline materials, can also be used to increase pH and add calcium, thereby decreasing water corrosivity [80; 38; 20].

Table 3. Summary Statistics of computed for industrial water quality index

	LSI	AI	PI
Number of values	55	55	55
Minimum	-3.22	8.61	3.84
Maximum	-0.03	11.89	8.31
Range	-1.27 - -3.22	8.61 - 11.89	3.84-8.31
Mean	-1.27	10.61	6.31
std. deviation	0.74	0.74	1.04

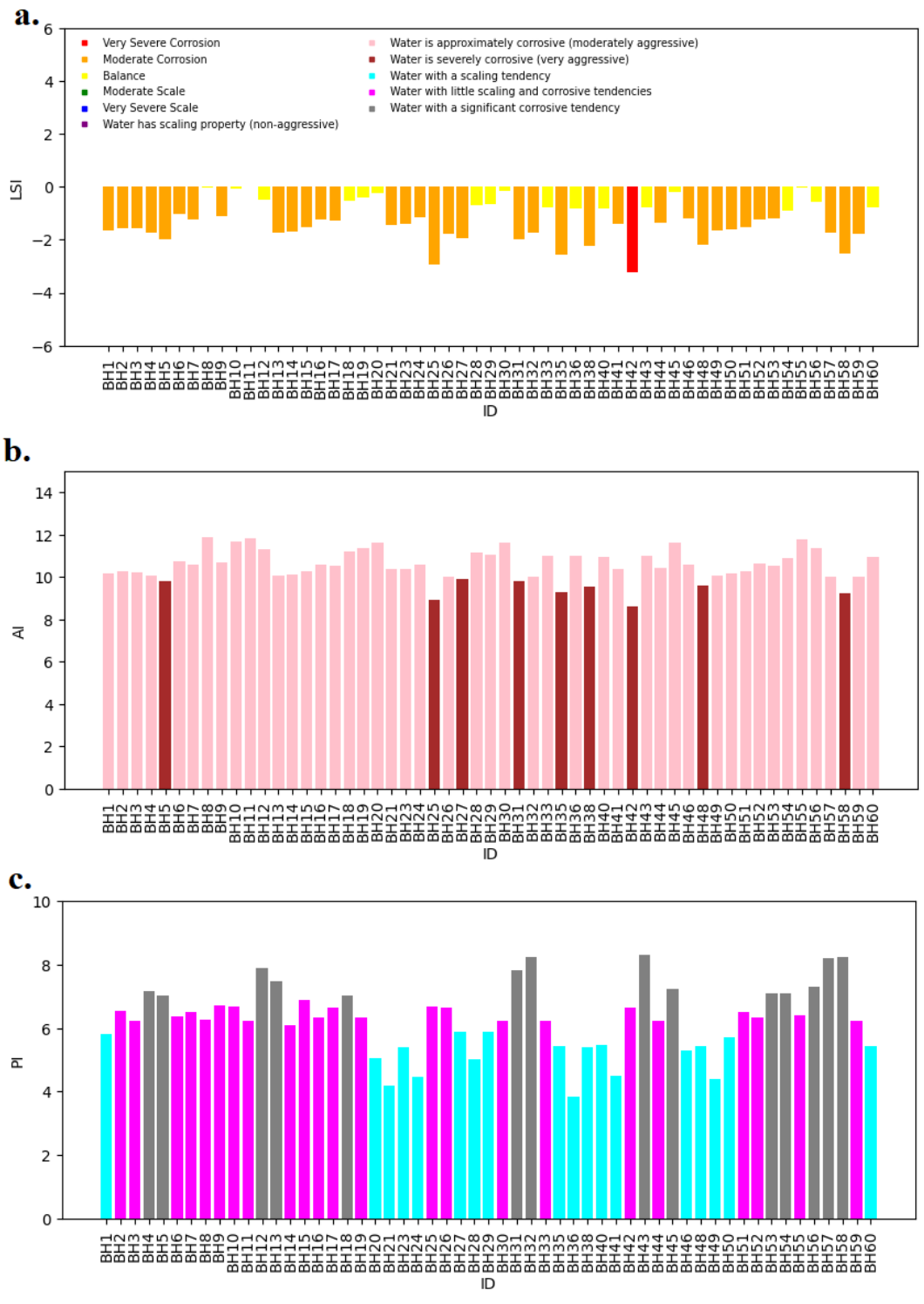

Figure 11. Distribution of (a) LSI, (b) AI, and PI in groundwater samples

CONCLUSION

The study reveals that the groundwater in the study area is predominantly acidic, with 80% of the samples having pH values below the WHO-recommended range of 6.5 to 8.5 for potable water. Despite the acidity, most other physicochemical properties of the groundwater samples fall within WHO standards for drinking water. The hydro-geochemical facies indicate that the groundwater is largely composed of Ca^{2+}+Mg^{2+}-HCO_3^- and Ca^{2+}+Mg^{2+}-SO_4^{2-}-Cl^- facies. The groundwater chemistry is influenced by rock-water interactions. Normal ion exchange dominates in the study area, with Na^+ and K^+ entering the groundwater from the surrounding aquifers. The saturation index (SI) of evaporitic minerals, such as calcite, anhydrite, gypsum, dolomite, and aragonite, shows these minerals are under-saturated, indicating no significant scaling. Additionally, the Revelle index confirms that seawater intrusion is not contributing to groundwater salinization. However, the industrial quality indices, including the Langelier Saturation Index, Aggressive Index, and Puckorius Index indicate moderate corrosivity and low scaling tendency, implying the groundwater may poses some risk to metallic industrial and municipal water systems. This suggests that mitigation strategies, such as the use of corrosion-resistant materials and water treatment solutions, are necessary to protect infrastructure from corrosion-related damage.

ACKNOWLEDGEMENT

The authors would like to thank their respective institutions for giving them the opportunity to conduct and carry out this research.

CONFLICT OF INTEREST

The authors declare no conflict of interest.

REFERENCES

[1] Abdelshafy, M., Saber, M., Abdelhaleem, A., Abdelrazek, S. M. and Seleem, E. M. (2019). Hydrogeochemical processes and evaluation of groundwater aquifer at Sohag city Egypt, Sci. Afr., 6: e00196. doi: 10.1016/j.sciaf.2019.e00196.

[2] Abubakar, H. O., Ige, O. O., Olatunji, S. and Iheme, K. O. (2023). Characterizing groundwater potentials in parts of the basement complex of Nigeria using GIS and remote sensing, Sustain. Water Resour. Manag., 9(2). doi: 10.1007/s40899-023-00826-1.

[3] Ahmed, S., Wajahat, S. M., Alam, M., Hussain, A., Qureshi, F. and Khurshid, S. (2020). Evaluation of corrosive behaviour and scaling potential of shallow water aquifer using corrosion indices and geospatial approaches in regions of the Yamuna river basin, J. King Saud Univ. Sci., 32: 101237. doi: 10.1016/j.jksus.2020.101237.

[4] Akakuru, O. C., Eze, C. U., Okeke, O. C., Opara, A. I., Usman, A. O., Iheme, O., Ibeneme, S. I. and Iwuoha, P. O. (2022). Hydrogeochemical evolution water quality indices irrigation suitability and pollution index of groundwater around eastern Niger Delta Nigeria, Int. J. Energy Water Resour. doi: 10.1007/s42108-021-00162-0.

[5] Alipour, V., Dindarloo, K., Mahvi, A. H. and Rezaei, L. (2014). Evaluation of corrosion and scaling tendency indices in a drinking water distribution system a case study of Bandar Abbas city Iran, J. Water Health, 13(1): 203–209. doi: 10.2166/wh.2014.157.

[6] Alley, W. M., Winter, T. C., Harvey, J. W. and Franke, O. L. (1998). Ground water and surface water a single resource, USGS Circ., 79.

[7] Amadi, A. N., Olasehinde, P. I. and Nwankwoala, H. O. (2014). Hydrogeochemistry and statistical analysis of Benin Formation in eastern Niger Delta Nigeria, Int. Res. J. Pure Appl. Chem., 4(3): 327–338. DOI: https://doi.org/10.9734/IRJPAC/2014/9154

[8] Aquatech (2019). Industrial water our essential guide to pollution treatment and solutions, Aquatech Trade

Publ. Available at: https://www.aquatechtrade.com/news/industrial-water/industrial-water-essential-guide/
[9] Akakuru O. C., Ray P. A., Soltanian M. R., Temgoua E., Eyankware M. O., Aigbadon G. O., Obite C. P., Algeo T. J., Akingboye A. S. (2025). Leveraging Novel Machine Learning Models in Predicting Groundwater Irrigation Suitability in Southeastern Nigeria: A Hydrogeochemical Approach, Scientific African, https://doi.org/10.1016/j.sciaf.2025.e02646
[10] Barzegar, R., Moghaddam, A. A., Tziritis, E., Fakhri, M. S. and Soltani, S. (2017). Identification of hydrogeochemical processes and pollution sources of groundwater resources in the Marand plain northwest of Iran, Environ. Earth Sci., 76: 297. doi: 10.1007/s12665-017-6612-y.
[11] Belkhiri, L., Boudoukha, A., Mouni, L. and Baouz, T. (2010). Application of multivariate statistical methods and inverse geochemical modeling for characterization of groundwater a case study Ain Azel plain Algeria, Geoderma, 159(3–4): 390–398. DOI: https://doi.org/10.1016/j.geoderma.2010.08.016
[12] Amadi CC, Okeke CO, Onyekuru SO, Okereke CN, Akakuru OC. (2025). Assessing groundwater pollution using advanced statistical techniques and pollution indices near a coal fly ash dump in parts of Oji-river, Nigeria. Environ Sci Pollut Res Int. Jul 7. doi: 10.1007/s11356-025-36672-1.
[13] Musa, K.O., Akpah, F.A., Akakuru, O.C. et al. Carcinogenic risk assessment, hydrogeochemical signatures, and irrigation suitability of groundwater within Ajaokuta and environs, North Central, Nigeria. Int J Energ Water Res 10, 9 (2026). https://doi.org/10.1007/s42108-025-00424-1
[14] Durov, S. A. (1948). Classification of natural waters and graphical representation of their composition, Dokl. Akad. Nauk USSR, 59: 87–90.
[15] Earthsoft (2020). Schoeller diagram, *Earthsoft Help Docs*. Available at: https://help.earthsoft.com/schoeller-diagram.
[16] EDMS (2020). What are Schoeller diagrams in geo chemistry, *Environ. Data Manag. Syst.* Available at: https://environmentalstandards.info/schoeller-diagrams-in-geo-chemistry/.
[17] Egbueri, J. C. (2019). Evaluation and characterization of the groundwater quality and hydrogeochemistry of Ogbaru farming district in southeastern Nigeria, *SN Appl. Sci.*, 1(8). doi: 10.1007/s42452-019-0853-1.
[18] Opara, A.I., Ireaja, A.N., Eyankware, M.O., Urom, O.O, Ikoro D.O, Akakuru, O.C, Dioha E, and Omoko N.E . A critical analysis of the comparative techniques of aquifer protective capacity studies in part of Southeastern Nigeria. Int J Energ Water Res (2023). https://doi.org/10.1007/s42108-023-00251-2
[19] Akakuru, O.C, Onyeanwuna, U.B, Opara A.I, Iheme, K.O, Njoku, A.O, Amadi, C.C, Akaolisa, C.C.Z1, Okwuosha O.R (2023). Electro-geohydraulic Estimation of Shallow Aquifer Characteristics of Njaba and Environs, Southeastern Nigeria. Arabian Journal of Geosciences 10.1007/s12517-023-11378-1
[20] Aghamelu, O. P., Eyankware, M. O., & Akakuru, O. C. (2025). Geochemical characterization and risk implications of groundwater for irrigation and drinking around the agrarian metropolis of southeastern Nigeria. Sustainable Water Resources Management, 11, 133. https://doi.org/10.1007/s40899-025-01305-5
[21] Eyankware, M. O., Mba-Otike, M. N., Odesa, G. E., Chukwusa, F. O., Osisanya, W. O., Eyankware-Ulakpa, R. O., Akakuru, O. C., & Komolafe, N. P. (2025). Saline intrusion in Niger Delta coastal aquifers, drivers, hydrogeological dynamics and mitigation strategies. Discover Geoscience, 3, 150. https://doi.org/10.1007/s44288-025-00264-w
[22] Adedibu Sunny Akingboye, Andy Anderson Bery, Abimbola Chris Ogunyele, Joseph Gnapragasan, Taiwo Adewumi, Anthony Victor Oyeshomo, Obinna Chigoziem Akakuru, Oluwatimilehin Balogun, (2025). Magneto-radiometric and geochemical mapping of structurally controlled hydrothermal gold mineralization in the Okpella Neoproterozoic terrain, Igarra Schist Belt, SW Nigeria, Scientific African. https://doi.org/10.1016/j.sciaf.2025.e02960.
[23] Eslamia, F., Salari, M., Yousefi, N. and Mahvi, A. H. (2020). Evaluation of quality scaling and corrosion potential of groundwater resources using stability index case study Kerman Province Iran, *Desalin. Water Treat.*, 179: 19–27. doi: 10.5004/dwt.2020.24999.
[24] Gaillardet, J., Dupré, B., Louvat, P. and Allegre, C. J. (1999). Global silicate weathering and CO2 consumption rates deduced from the chemistry of large rivers, *Chem. Geol.*, 159: 3–30. doi: 10.1016/S0009-2541(99)00031-5.
[25] Ofoh, I. J., Onyekuru, S. O., Ikoro, D. O., Opara, A. I., Okoro, E. M., Okereke, C. N., & Akakuru, O. C. (2025). Enhanced reservoir characterization of the "IFY" field offshore Niger Delta Basin using well logs and seismic data. Petroleum and Coal. https://www.vurup.sk/doi:10.14232/petcoal2023v65n3.
[26] Gibbs, R. J. (1970). Mechanisms controlling world water chemistry, *Science*, 170: 1088–1090.
[27] GISGeography (2022). Inverse distance weighting IDW interpolation, *GISGeography*. Available at: https://gisgeography.com/inverse-distance-weighting-idw-interpolation/.
[28] Goldensoftware (2019). What is a piper plot trilinear diagram, *Golden Software Support*. Available at: https://support.goldensoftware.com/hc/en-us/articles/115003101648.
[29] Hack (2008). Langelier and aggressive indices method 8073, *Hack Water Technol.* Available at: https://stpnq.com/wp-content/uploads/2014/08/Langelier-index.pdf.
[30] Onyekuru, S. O., Anyanwu, T. C., Nwosu, K. O., Ofoh, I. J., Akiang, F. B., Akakuru, O. C., Achukwu–Ononye, O. U., Ibe, K. K., & Aigbadon, G. O. (2025). https://www.vurup.sk/doi:10.14232/petcoal2023v65n3Energy Geoscience, in press. https://doi.org/10.1016/j.engeos.2025.100447
[31] Eyankware MO, Akakuru OC, Inoni OE, Osisanya WO, Ukor KP, Umuokoro G (2025). Interpretation of hydrochemical data in selected parts of Warri, Southern Nigeria using health risk assessment and heavy metal

index. Discovery Nature 2025; 2: e6dn3107 doi: https://doi.org/10.54905/disssi.v2i3.e6dn3107
[32] Akakuru, O.C., Eyankware, M.O., Aigbadon, G.O. et al. Carcinogenic health risks and water quality assessment of groundwater around lead–zinc mining areas of Ebonyi state Nigeria: a data-driven machine learning approach. Discov Civ Eng 1, 130 (2024). https://doi.org/10.1007/s44290-024-00134-3
[33] Najar, I. N., Sharma, P., Das, S., Sherpa, M. T., Kumar, S., & Thakur, N. (2022). *Bacterial diversity, physicochemical and geothermometry of South Asian hot springs*. Current Research in Microbial Sciences, 3, 100125. https://doi.org/10.1016/j.crmicr.2022.100125
[34] Kumar, V. S., Amarender, B., Dhakate, R., Sankaran, S., & Kumar, K. R. (2016). Assessment of groundwater quality for drinking and irrigation use in shallow hard rock aquifer of Pudunagaram, Palakkad District, Kerala. *Applied Water Science*, **6**(2), 149–167. https://doi.org/10.1007/s13201-014-0239-6
[35] Langelier, W. F. (1936). The analytical control of anti corrosion water treatment, *J. Am. Water Works Assoc.*, 28: 1500.
[36] Lenntech (2022). Ryznar stability index calculator, *Lenntech Water Treat.* Available at: https://www.lenntech.com/calculators/ryznar/index/ryznar.htm.
[37] Lloyd, J. A. and Heathcote, J. A. (1985). Natural inorganic hydrochemistry in relation to groundwater an introduction, *Oxford Univ. Press*, New York: 296.
[38] Mahamat Nour, A., Vallet Coulomb, C., Bouchez, C., Ginot, P., Doumnang, J. C., Sylvestre, F. and Deschamps, P. (2019). Geochemistry of the Lake Chad tributaries under strongly varying hydro climatic conditions, *Aquat. Geochem.* doi: 10.1007/s10498-019-09363-w.
[39] Marandi, A. and Shand, P. (2018). Groundwater chemistry and the Gibbs diagram, *Appl. Geochem.* doi: 10.1016/j.apgeochem.2018.07.009.
[40] Mbaegbu, G. I., Ihem, E. E., Okon, M. A., & Akakuru, O. C. (2024). Impact of waste dumps on soil and groundwater quality in Owerri, Southeastern Nigeria. Agriculture, Food, and Natural Resources Journal, 3(1), 113–121. https://doi.org/10.5281/zenodo.13932188
[41] Usman, A.O., Akakuru, O.C., Azuoko, GB. et al. Enhancing aquifer protective capacity prediction over Ibeator and environ, Southeastern Nigeria using artificial neural networks and multivariate linear regression analysis. BMC Environ Sci 1, 13 (2024). https://doi.org/10.1186/s44329-024-00013-3
[42] Naus, C. A., Driscoll, D. G., & Carter, J. M. (2001). Geochemistry of the Madison and Minnelusa aquifers in the Black Hills area, South Dakota. Water-Resources Investigations Report 2001-4129. U.S. Geological Survey. https://doi.org/10.3133/wri014129
[43] Négrel, P., Allègre, C. J., Dupré, B. and Lewin, E. (1993). Erosion sources determined by inversion of major and trace element ratios and strontium isotopic ratios in river water the Congo Basin case, *Earth Planet. Sci. Lett.*, 120: 59–76. doi: 10.1016/0012-821X(93)90023-3.
[44] Eyankware, M.O, Akakuru, O.C., Igwe, E.O. et al. Pollution Indices, Potential Ecological Risks and Spatial distribution of Heavy Metals in soils around Delta State, Nigeria. Water Air Soil Pollut 235, 452 (2024). https://doi.org/10.1007/s11270-024-07209-y
[45] Obiefuna, G. I., Dio, C. J., Lakuza, A. J., & Seli, A. B. (2019). Physicochemical characteristics of groundwater quality of Dumne area, northeast Nigeria. International Journal of Advanced Engineering Research and Science, 6(3), 261–276. https://doi.org/10.22161/ijaers.6.3.35
[46] Ogbozige, F. J. and Toko, M. A. (2020). Piper trilinear and Gibbs description of groundwater chemistry in Port Harcourt Nigeria, *Appl. Sci. Eng. Prog.*, 13(4): 362–369. doi: 10.14416/j.asep.2020.08.003.
[47] Okpoli, C. C., & Iselowo, D. O. (2019). Hydrogeochemistry of Lekki, Ajah and Ikorodu water resources, southwestern Nigeria. Journal Clean WAS, 3(2), 20–24. https://doi.org/10.26480/jcleanwas.02.2019.20.24
[48] Omar, W., Chen, J. and Ulrich, J. (2010). Reduction of seawater scale forming potential using the fluidized bed crystallization technology, *Desalination*, 250(1): 95–100. doi: 10.1016/j.desal.2009.03.013.
[49] Aigbadon, G.O, Chinyem, F.I, Alege,T.S, Overare,B, Akakuru, O.C et al. (2024). Outcrops as windows to petroleum systems: Insights from the southern Bida Basin, Nigeria, Energy Geoscience, 5 (3), https://doi.org/10.1016/j.engeos.2024.100294
[50] Parkhurst, D. L., & Appelo, C. A. J. (1999). User's guide to PHREEQC (Version 2)—A computer program for speciation, batch-reaction, one-dimensional transport, and inverse geochemical calculations (Water-Resources Investigations Report 99-4259). U.S. Geological Survey. https://doi.org/10.3133/wri994259
[51] Parkhurst, D. L., & Appelo, C. A. J. (1999). User's guide to PHREEQC (Version 2): A computer program for speciation, batch-reaction, one-dimensional transport, and inverse geochemical calculations (Water-Resources Investigations Report 99-4259). U.S. Geological Survey. https://doi.org/10.3133/wri994259
[52] Peterside, A. N., Hart, A. I., & Nwankwoala, H. O. (2022). Groundwater quality for irrigation purposes and classification for hydrochemical facies in parts of Southern Ijaw Local Government Area, Bayelsa State, Nigeria. Journal of Environmental Protection, 13(4), 315–330. https://doi.org/10.4236/jep.2022.134020
[53] Picouet, C., Dupré, B., Orange, D. and Valladon, M. (2002). Major and trace element geochemistry in the upper Niger River Mali physical and chemical weathering rates and CO2 consumption, *Chem. Geol.*, 185: 93–124. doi: 10.1016/S0009-2541(01)00398-9.
[54] Piper, A. M. (1944). A graphical procedure in the geochemical interpretation of water analysis, *Trans. Am. Geophys. Union*, 25: 914–928.
[55] Udeh, H.M., Opara, A.I., Akakuru, O.C. et al. (2024). Aquifer geo-hydraulic characteristics of Enugu and

environs, southeastern Nigeria using pumping test and geo-sounding data. Int J Energ Water Res https://doi.org/10.1007/s42108-024-00304-0 .
[56] Raj, D. and Shaji, E. (2017). Fluoride contamination in groundwater resources of Alleppey southern India, *Geosci. Front.*, 8: 117–124. doi: 10.1016/j.gsf.2016.01.002.
[57] Raju, N. J., Chaudhary, A., Nazneen, S., Singh, S., & Goyal, A. (2015). Hydrogeochemical investigation and quality assessment of groundwater for drinking and agricultural use in JNU, New Delhi, India. In Management of Natural Resources in a Changing Environment (pp. 3–27). Springer. https://doi.org/10.1007/978-3-319-12559-6_1
[58] Revelle, R. (1941). Criteria for recognition of seawater in groundwater, *Trans. Am. Geophys. Union*, 22: 593–597.
[59] Ryznar, J. W. (1944). A new index for determining the amount of calcium carbonate scale formed by a water, *J. Am. Water Works Assoc.*, 36: 472–475.
[60] Sajil Kumar, P. J. (2019). Assessment of corrosion and scaling potential of the groundwater in the Thanjavur district using hydrogeochemical analysis and spatial modeling techniques, *SN Appl. Sci.*, 1(5): 395. doi: 10.1007/s42452-019-0423-6.
[61] Sargazi, S., Almodaresi, S. A., Ebrahimi, A. A., Dalvand, A., Sargazi, H., & Khatebasreh, M. (2020). Assessment of groundwater quality for industrial purposes using geographical information system in Zahedan, Sistan and Baluchestan Province, Iran. Journal of Environmental Health and Sustainable Development, 5(4), 1162–1172. https://doi.org/10.18502/jehsd.v5i4.4968
[62] Schoeller, H. (1967). Geochemistry of groundwater an international guide for research and practice, *UNESCO*, Chap. 15: 1–18.
[63] Schoeller, H. (1962). Geochemie des eaux souterraines, *Rev. Inst. Fr. Pétrole*, 10: 230–244.
[64] Sheikhy, N. T., Ramli, M. F., Aris, A. Z., Sulaiman, W. A., Juahir, H. and Fakharian, K. (2014). Identification of the hydrogeochemical processes in groundwater using classic integrated geochemical methods and geostatistical techniques in Amol Babol plain Iran, *Sci. World J.*, 2014: 1–15. doi: 10.1155/2014/419058.
[65] Shukla, T., Sundriyal, S., Stachnik, L. and Mehta, M. (2018). Carbonate and silicate weathering in glacial environments and its relation to atmospheric CO2 cycling in the Himalaya, *Ann. Glaciol.*, 59(77): 159–170. doi: 10.1017/aog.2019.5.
[66] Usman,A.O, Abraham, E.M, Ezeh, C.C, Azuoko, G, Chinwuko, A.I, Chizoba, C.J., Akakuru, O.C (2024). Structural modelling of subsurface geologic structures in Anambra and adjoining Bida Basins using aeromagnetic data: Implications for mineral explorations., Kuwait Journal of Science,100307, https://doi.org/10.1016/j.kjs.2024.100307.
[67] Slavíčková, K., Grünwald, A. and Šťastný, B. (2013). Monitoring of the corrosion of pipes used for the drinking water treatment and supply, *Civ. Eng. Archit.*, 1(3): 61–65. doi: 10.13189/cea.2013.010302.
[68] Sunkari, E. D., Abu, M. and Zango, M. S. (2021). Geochemical evolution and tracing of groundwater salinization using different ionic ratios multivariate statistical and geochemical modeling approaches in a typical semi arid basin, *J. Contam. Hydrol.*, 236: 103742. doi: 10.1016/j.jconhyd.2020.103742.
[69] Udeh, H.M., Opara, A.I., Akakuru, O.C. et al. (2024). Assessment of Aquifer Vulnerability and Soil Corrosivity in Enugu and Environs, Southeastern Nigeria: Insights from Geo-Sounding Data. Polytechnica 7, 10. https://doi.org/10.1007/s41050-024-00050-6
[70] Udo, I., & Udofia, P. A. (2020). Petrography and provenance analysis of conglomeratic lithofacies of the Ameki Formation in northeastern part of the Niger Delta Basin, Nigeria. International Journal of Engineering Science, 9(6), 42–55. https://doi.org/10.9790/1813-0906024255
[71] Aigbadon, G.O., Igwe, E.O., Akakuru, O.C. et al. (2024) Sedimentological, palynostratigraphic investigation and paleoenvironmental reconstruction of the Chad Formation, Bornu (Chad) Basin Nigeria. Journal of Paleolimnology https://doi.org/10.1007/s10933-023-00308-6
[72] Vegesna, S. R. and McAnally, S. A. (1995). Corrosion indices as a method of corrosion measurement and a systems operating tool, *J. Environ. Sci. Health A*, 30(3): 583–605. doi: 10.1080/10934529509376219.
[73] Nwankwoala, H. O., Oyegun, V. O., Azuonwu, O., Okujagu, D. C., Ohwoghere-Asumad, O., & Akakuru, O. C. (2024). Trace metal concentrations and physico-chemical characteristics of groundwater around Ikwe-Ona refinery and surrounding environment, Akwa Ibom State, Nigeria. Environmental Contaminants Reviews, 1, 43–53. https://doi.org/10.26480/ecr.01.2024.43.53
[74] Vincy, M. V., Brilliant, R. and Pradeepkumar, A. P. (2014). Hydrochemical characterization and quality assessment of groundwater for drinking and irrigation purposes a case study of Meenachil River Basin Western Ghats Kerala India, *Environ. Monit. Assess.*, 187(1). doi: 10.1007/s10661-014-4217-4.
[75] WHO (2013). Drinking water quality guidelines 4th edn, *World Health Organ.*, Geneva Switzerland.
[76] Yousefi, Z., Kazemi, F. and Mohammadpour, R. A. (2016). Assessment of scale formation and corrosion of drinking water supplies in Ilam City Iran, *Environ. Health Eng. Manag. J.*, 3(2): 75–80. doi: 10.15171/EHEM.2016.04.
[77] Yusuf, M. A. (2020). Application of integrated methods to assess and characterise the hydrogeology of coastal aquifers in parts of Lagos southwest Nigeria, *PhD Thesis*.
[78] Yusuf, M. A., Abiye, T. A., Butler, M. J. and Ibrahim, K. O. (2018). Origin and residence time of shallow groundwater resources in Lagos coastal basin south west Nigeria an isotopic approach, *Heliyon*, 4(11): e00932.

doi: 10.1016/j.heliyon.2018.e00932.
[79] Zhang, B., Zhao, D., Zhou, P., Qu, S., Liao, F. and Wang, G. (2020). Hydrochemical characteristics of groundwater and dominant water rock interactions in the Delingha area Qaidam Basin northwest China, *Water*, 12(3): 836. doi: 10.3390/w12030836.
[80] Zhang, X., Zhao, R., Wu, X. and Mu, W. (2021). Hydrogeochemistry identification of hydrogeochemical evolution mechanisms and assessment of groundwater quality in the southwestern Ordos Basin China, *Environ. Sci. Pollut. Res.* doi: 10.1007/s11356-021-15643-2.
[81] DRINKING WATER (2019). Drinking water contaminant corrosive water, *Drinking Water Ext*. Available at: https://drinking-water.extension.org/drinkingwatercontaminantcorrosivewater/.
[82] Juliana, O., Okechuwu, O., Diugo, I., Iheanyichukwu, O., I.O, N., Chikwendu, O., & Akakuru C. (2024). Enhancing Facies Classification in Geological Studies Through Artificial Neural Networks: A Review. Sustainable Earth Trends, 3(4), 31-45. doi: 10.48308/ser.2024.234950.1041